

**Supplementary Materials**  
for  
**Luminescent diimine-Pt(IV) complexes with axial phenyl selenide ligands**

Marzieh Dadkhah Aseman<sup>a\*</sup>, Reza Babadi Aghakhanpour<sup>a</sup>, Zohreh Sharifioliae<sup>b</sup>, Axel Klein<sup>c</sup>\*  
and S. Masoud Nabavizadeh<sup>d</sup>

<sup>a</sup> Department of Chemistry, Faculty of Sciences, Tarbiat Modares University, Tehran, 15719-14911, Iran,  
Email: m.dadkhah@modares.ac.ir

<sup>b</sup> Faculty of Chemistry, Kharazmi University, Tehran 15719-14911, Iran.

<sup>c</sup> University of Cologne, Faculty of Mathematics and Natural Sciences, Department of Chemistry, Institute  
for Inorganic Chemistry, Greinstrasse 6, D-50939 Köln, Germany, Email: axel.klein@uni-koeln.de

<sup>d</sup> Professor Rashidi Laboratory of Organometallic Chemistry, Department of Chemistry, College of  
Sciences, Shiraz University, Shiraz 71467-13565, Iran

---

## Contents

**Figure S1.**  $^1\text{H}$  NMR spectrum of **1b** in  $\text{CDCl}_3$ .

**Figure S2.**  $^1\text{H}$  NMR spectrum of **2b** in  $\text{CDCl}_3$ .

**Figure S3.**  $^1\text{H}$  NMR spectrum of **3b** in  $\text{CDCl}_3$ .

**Figure S4.**  $^{13}\text{C}\{\text{H}\}$  NMR spectrum of **3b** in  $\text{CDCl}_3$ .

**Figure S5.**  $^{77}\text{Se}\{\text{H}\}$  NMR spectrum of **3b** in  $\text{CDCl}_3$ .

**Figure S6.** View of the DFT-optimised  $S_0$  structure of **1b** in the gas phase with atom numbering.

**Table S1.** Selected DFT-calculated metrics for the  $S_0$  state of **1b** in the gas phase and  $\text{CH}_2\text{Cl}_2$  compared with  
experimental data from single crystal XRD.

**Table S2.** Selected DFT-calculated metrics for the  $T_1$  state of the complexes **1b** and **2b** in the gas phase.

**Figure S7.** View of the DFT-optimised  $S_0$  structure of **2b** in the gas phase with atom numbering.

**Table S3.** Selected DFT-calculated metrics for the  $S_0$  state of **2b** in the gas phase and  $\text{CH}_2\text{Cl}_2$  compared with  
experimental data from single crystal XRD.

**Figure S8.** View of the DFT-optimised  $S_0$  structure of **3b** in the gas phase with atom numbering.

**Table S4.** Selected DFT-calculated metrics for the  $S_0$  state of **3b** in gas phase and  $\text{CH}_2\text{Cl}_2$ .<sup>a</sup>

**Figure S9.** UV-vis absorption spectra of **1b**, **2b**, **3b** (all  $10^{-5}$  M) in  $\text{CH}_2\text{Cl}_2$  at 298 K.

**Figure S10.** UV-vis absorption spectra of the complex **3b** in *tris*-HCl buffer at 298 K ( $1.1 \times 10^{-5}$  M). blue line,  
 $t = 0$ , red line,  $t = 30$  min.

**Figure S11.** Molecular orbital plots for the DFT-optimised  $S_0$  structure of **1b** in  $\text{CH}_2\text{Cl}_2$  solution.

**Figure S12.** Molecular orbital plots for the DFT-optimised  $S_0$  structure of **2b** in  $\text{CH}_2\text{Cl}_2$  solution.

**Figure S13.** Molecular orbital plots for the DFT-optimised  $S_0$  structure of **3b** in  $\text{CH}_2\text{Cl}_2$  solution.

**Table S5.** Composition and energies of selected molecular orbitals of **1b** in  $\text{CH}_2\text{Cl}_2$ .

**Table S6.** Composition and energies of selected molecular orbitals of **2b** in  $\text{CH}_2\text{Cl}_2$ .

**Table S7.** Composition and energies of selected molecular orbitals of **3b** in  $\text{CH}_2\text{Cl}_2$ .

**Table S8.** Wavelengths and the nature of transitions for the complex **1b**.

**Table S9.** Wavelengths and the nature of transitions for the complex **2b**.

**Table S10.** Wavelengths and the nature of transitions for the complex **3b**.

---

## References

---

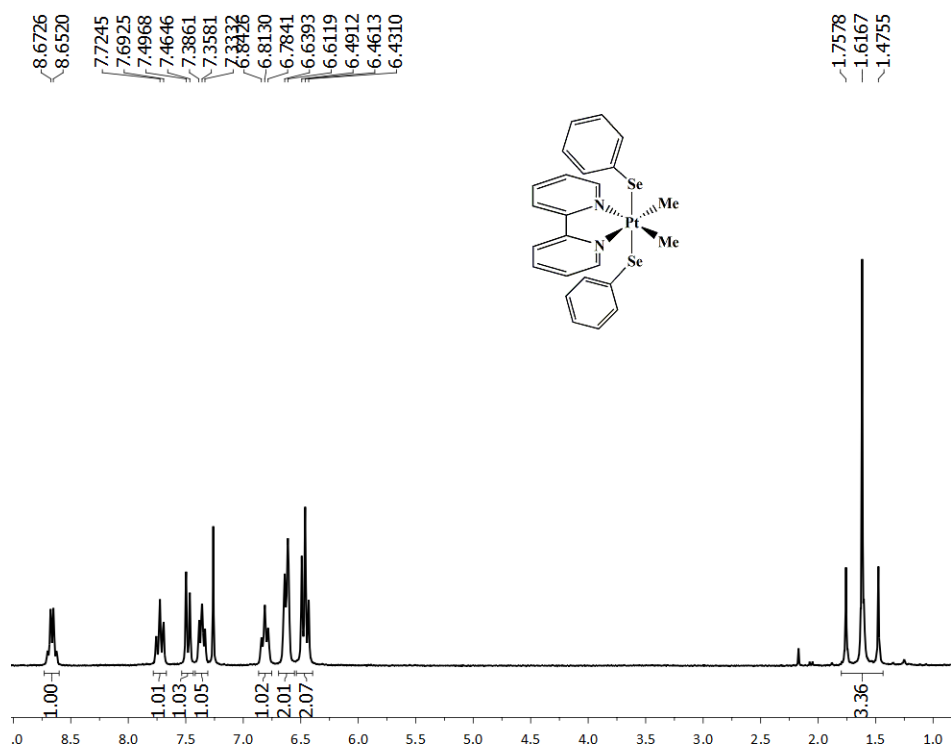


**Figure S1.** <sup>1</sup>H NMR spectrum of **1b** in  $\text{CDCl}_3$ .

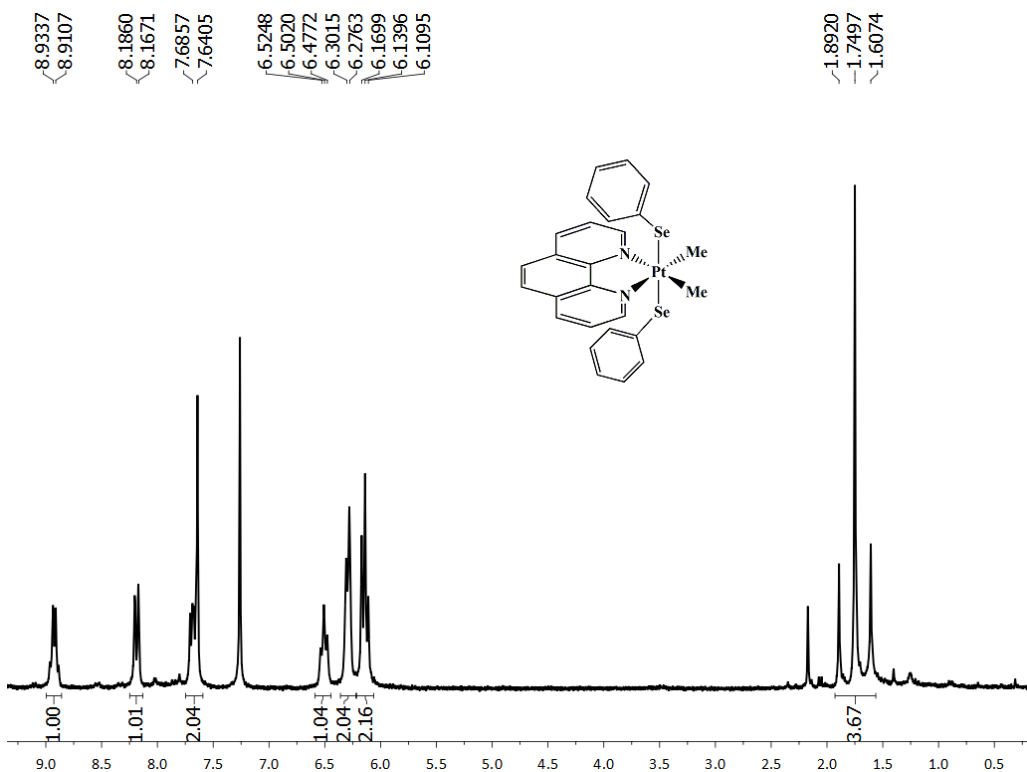


**Figure S2.** <sup>1</sup>H NMR spectrum of **2b** in  $\text{CDCl}_3$ .

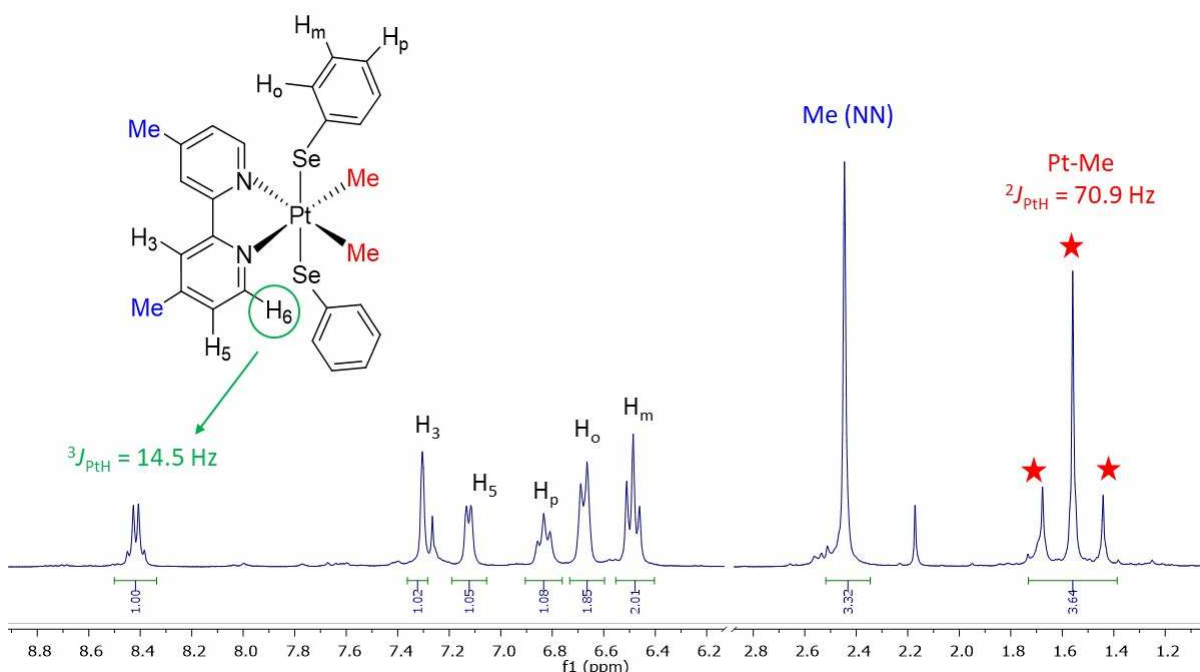


**Figure S3.**  $^1\text{H}$  NMR spectrum of **3b** in CDCl<sub>3</sub>.

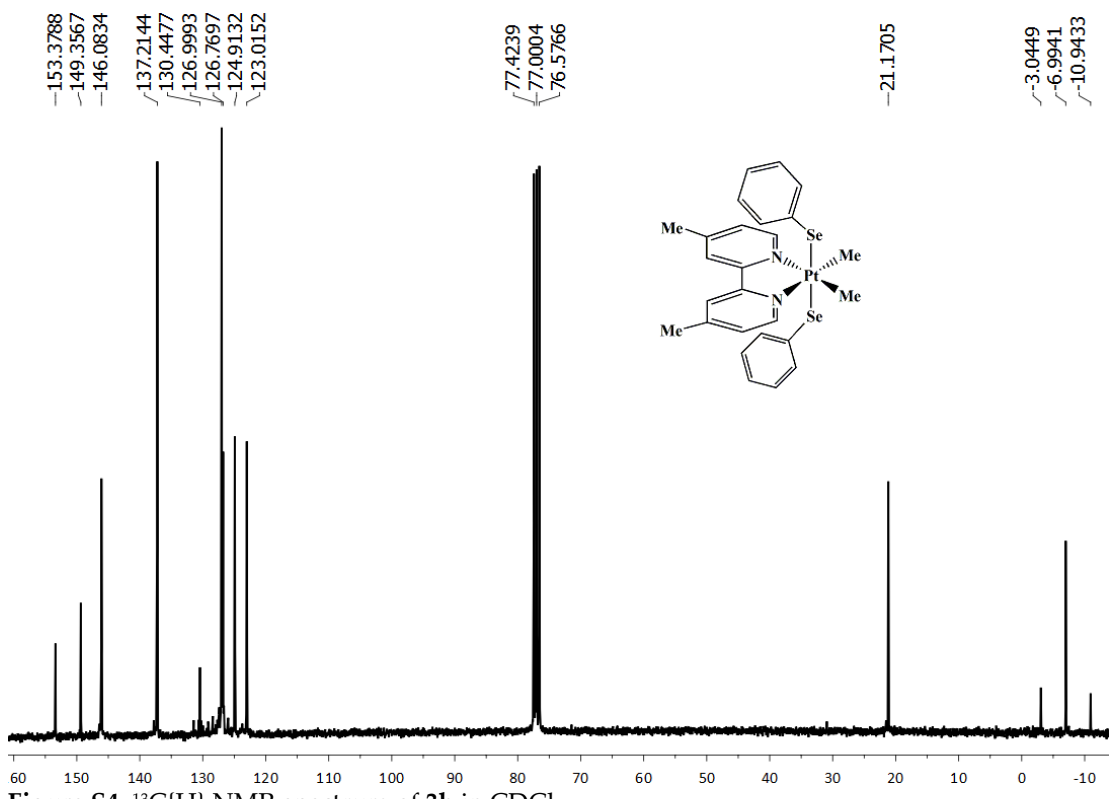


**Figure S4.**  $^{13}\text{C}\{\text{H}\}$  NMR spectrum of **3b** in CDCl<sub>3</sub>.

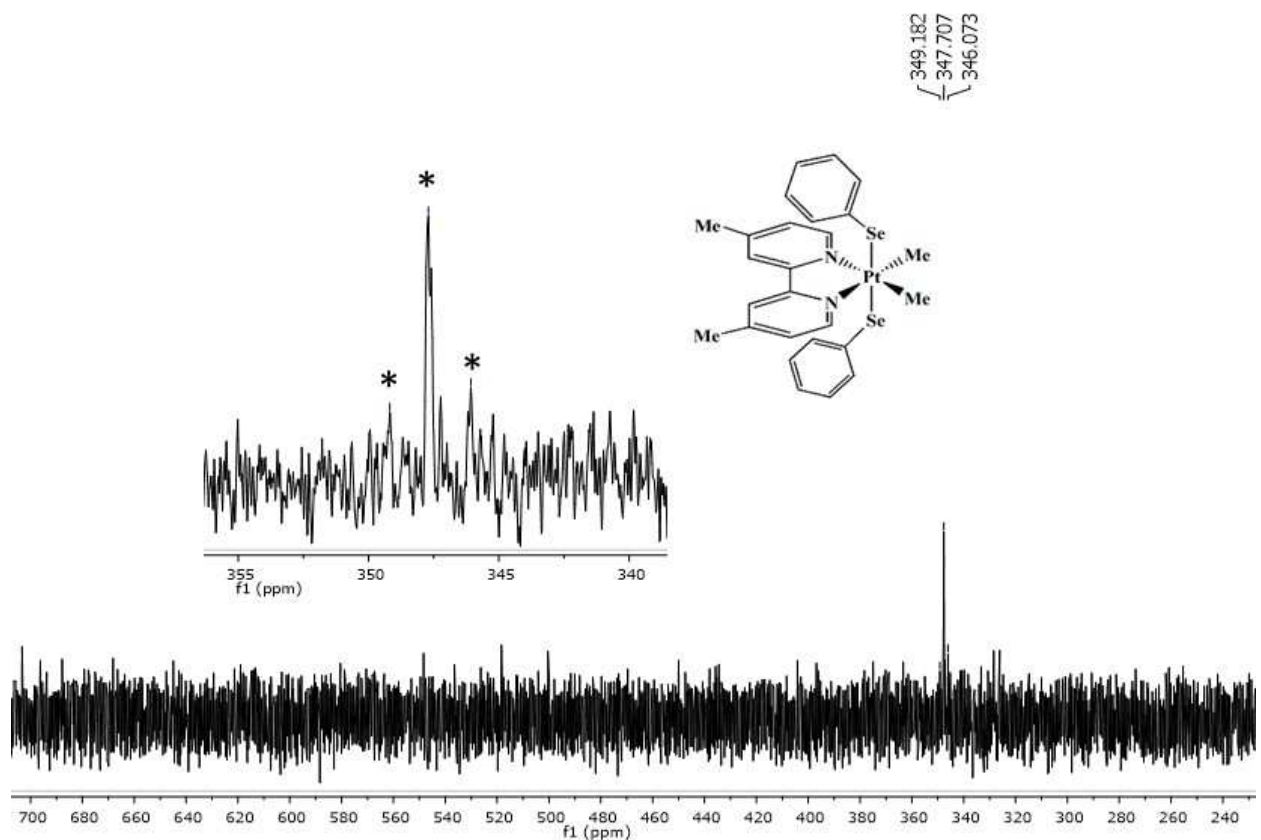


**Figure S5.**  $^{77}\text{Se}\{\text{H}\}$  NMR spectrum of **3b** in  $\text{CDCl}_3$ .

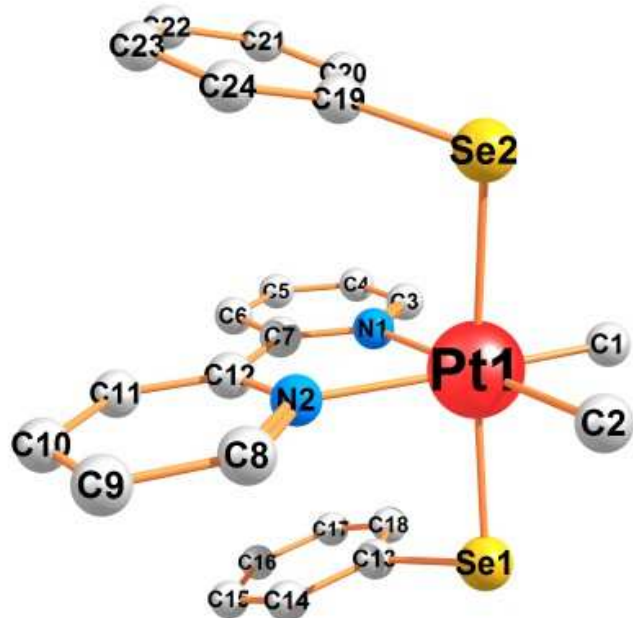


**Figure S6.** View of the DFT-optimised  $S_0$  structure of **1b** in the gas phase with atom numbering.

**Table S1.** Selected DFT-calculated metrics for the  $S_0$  state of **1b** in the gas phase and  $\text{CH}_2\text{Cl}_2$  <sup>a</sup> compared with experimental data from single crystal XRD.

distances (Å)	$S_0$ (gas phase)	$S_0$ ( $\text{CH}_2\text{Cl}_2$ )	experimental <sup>b</sup>
Pt1–Se1	2.629	2.629	2.478(1)
Pt1–Se2	2.626	2.625	2.498(1) <sup>c</sup>
Pt1–N1	2.256	2.250	2.162(5) <sup>c</sup>
Pt1–N2	2.223	2.216	2.162(5)
Pt1–C1	2.078	2.081	2.055(8)
Pt1–C2	2.071	2.074	2.055(8)
angles (°)			
N1–Pt1–N2	74.075	74.530	76.4(2)
C2–Pt1–C1	85.740	85.577	86.6(3)
N2–Pt1–C2	98.319	98.230	98.5(3)
C1–Pt1–N1	101.921	101.696	98.5(3)
C1–Pt1–N2	175.665	176.051	174.9(3)
C2–Pt1–N1	172.119	172.556	174.9(3)
Pt–Se1–C13	105.302	106.119	103.4(4)
Pt–Se2–C19	104.993	105.891	103.1(3)
Se1–Pt1–Se2	172.501	172.499	173.24(4)

<sup>a</sup> DFT-calculated geometries on B3LYP level of theory, LANL2DZ basis sets for Pt and Se, 6-31G(d) basis sets for C, H, and N. <sup>b</sup> From ref. 1. <sup>c</sup> Different values to disorder.

**Table S2.** Selected DFT-calculated metrics for the  $T_1$  state of the complexes **1b** and **2b** in the gas phase.

<b>1b</b>		<b>2b</b>	
distances (Å)	$T_1$ (gas phase)	distances (Å)	$T_1$ (gas phase)
Pt1–Se1	3.166	Pt1–Se1	3.120
Pt1–Se2	3.035	Pt1–Se2	3.119
Pt1–N1	2.241	Pt1–N1	2.236
Pt1–N2	2.214	Pt1–N2	2.236
Pt1–C1	2.058	Pt1–C1	2.053
Pt1–C2	2.053	Pt1–C2	2.053
angles (°)		angles (°)	
N1–Pt1–N2	74.552	N1–Pt1–N2	75.458
C2–Pt1–C1	86.152	C2–Pt1–C1	86.182
N2–Pt1–C2	97.471	N2–Pt1–C2	99.180
C1–Pt1–N1	101.812	C1–Pt1–N1	99.183
C1–Pt1–N2	176.200	C1–Pt1–N2	174.607
C2–Pt1–N1	172.006	C2–Pt1–N1	174.603
Pt–Se1–C13	106.161	Pt–Se1–C15	102.566
Pt–Se2–C19	105.471	Pt–Se2–C21	102.565
Se1–Pt1–Se2	157.672	Se1–Pt1–Se2	157.325

<sup>a</sup> DFT-calculated geometries on B3LYP level of theory, LANL2DZ basis sets for Pt and Se, 6-31G(d) basis sets for C, H, and N.

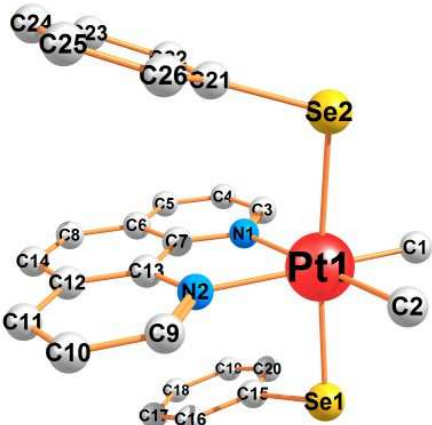


**Figure S7.** View of the DFT-optimised  $S_0$  structure of **2b** in the gas phase with atom numbering.

**Table S3.** Selected DFT-calculated metrics for the  $S_0$  state of **2b** in the gas phase and  $\text{CH}_2\text{Cl}_2$  <sup>a</sup> compared with experimental data from single crystal XRD.

distances (Å)	$S_0$ (gas phase)	$S_0$ ( $\text{CH}_2\text{Cl}_2$ )	exp. I <sup>b</sup>	exp. II <sup>c</sup>	exp. II <sup>d</sup>
Pt1–Se1	2.628	2.627	2.491(1)	2.4896(9)	2.495(3)
Pt1–Se2	2.624	2.627	2.486(1)	2.4896(9)	2.495(3)
Pt1–N1	2.254	2.247	2.150(5)	2.143(6)	2.120(18)
Pt1–N2	2.241	2.247	2.168(6)	2.143(6)	2.120(18)
Pt1–C1	2.073	2.077	2.058(9)	2.056(8)	2.092(20)
Pt1–C2	2.073	2.077	2.049(8)	2.056(8)	2.092(20)
angles (°)					
N1–Pt1–N2	74.921	74.910	77.2(2)	77.2(2)	75.0(7)
C2–Pt1–C1	86.062	84.965	85.7(3)	85.6(3)	87.4(9)
N2–Pt1–C2	98.767	100.052	98.0(3)	98.6(3)	98.8(8)
C1–Pt1–N1	100.370	100.088	99.0(3)	98.6(3)	87.4(9)
C1–Pt1–N2	174.618	174.902	175.2(3)	175.8(3)	173.8(8)
C2–Pt1–N1	173.061	174.863	176.2(3)	175.8(3)	173.8(8)
Pt–Se1–C15	104.855	106.218	105.1(1)	103.7(2)	106.9(5)
Pt–Se2–C21	104.796	106.229	104.2(2)	103.7(2)	106.9(5)
Se1–Pt1–Se2	174.275	173.657	173.82(3)	174.70(3)	175.4(1)

<sup>a</sup> DFT-calculated geometries on B3LYP level of theory, LANL2DZ basis sets for Pt and Se, 6-31G(d) basis sets for C, H, and N. <sup>b</sup> From ref. 1, triclinic space group c From ref. 1 tetragonal. <sup>d</sup> From Ref. 2.

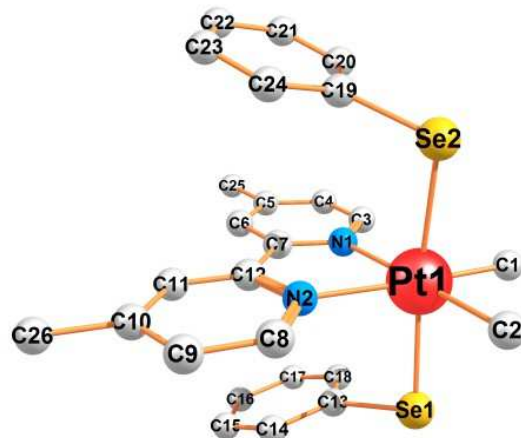


**Figure S8.** View of the DFT-optimised  $S_0$  structure of **3b** in the gas phase with atom numbering.

**Table S4.** Selected DFT-calculated metrics for the  $S_0$  state of **3b** in gas phase and  $\text{CH}_2\text{Cl}_2$ .<sup>a</sup>

distances (Å)	$S_0$ (gas phase)	$S_0$ ( $\text{CH}_2\text{Cl}_2$ )
Pt1–Se1	2.629	2.629
Pt1–Se2	2.627	2.626
Pt1–N1	2.252	2.247
Pt1–N2	2.221	2.213
Pt1–C1	2.078	2.080
Pt1–C2	2.071	2.074
angles (°)		
N1–Pt1–N2	73.991	74.448
N2–Pt1–C2	98.417	98.164
C2–Pt1–C1	86.092	85.786
C1–Pt1–N1	101.550	101.629
C1–Pt1–N2	175.251	175.943
C2–Pt1–N1	172.173	172.430
Pt–Se1–C13	105.373	106.217
Pt–Se2–C19	105.083	105.836
Se1–Pt1–Se2	172.536	172.460

<sup>a</sup> DFT-calculated geometries on B3LYP level of theory, LANL2DZ basis sets for Pt and Se, 6-31G(d) basis sets for C, H, and N.

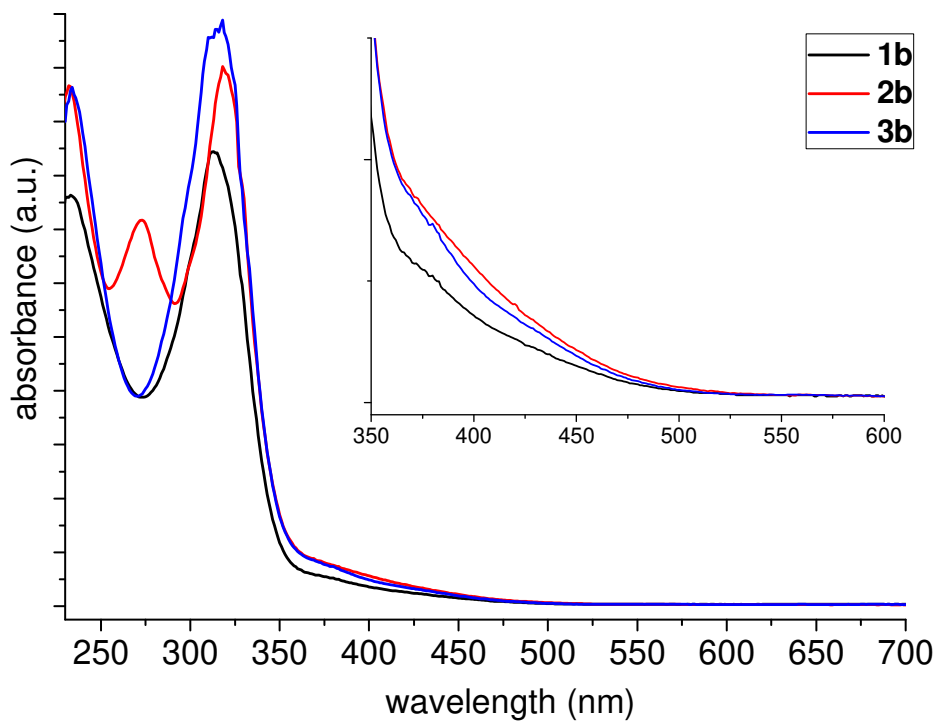


**Figure S9.** UV-vis absorption spectra of **1b** (black), b) **2b** (red) and c) **3b** (blue) (all  $10^{-5}$  M) in  $\text{CH}_2\text{Cl}_2$  at 298 K. Inset: Expanded spectra in the wavelength range 350–600 nm.

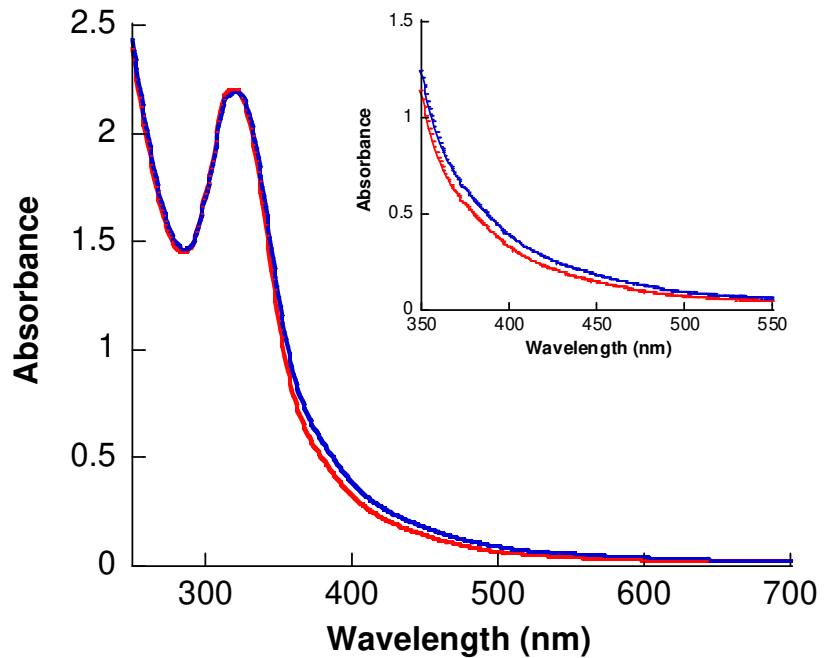


**Figure S10.** UV-vis absorption spectra of the complex **3b** in *tris*-HCl buffer at 298 K ( $1.1 \times 10^{-5}$  M); blue line,  $t = 0$ , red line,  $t = 30$  min (in the dark). Inset: Expanded spectra in the wavelength range 350–550 nm.

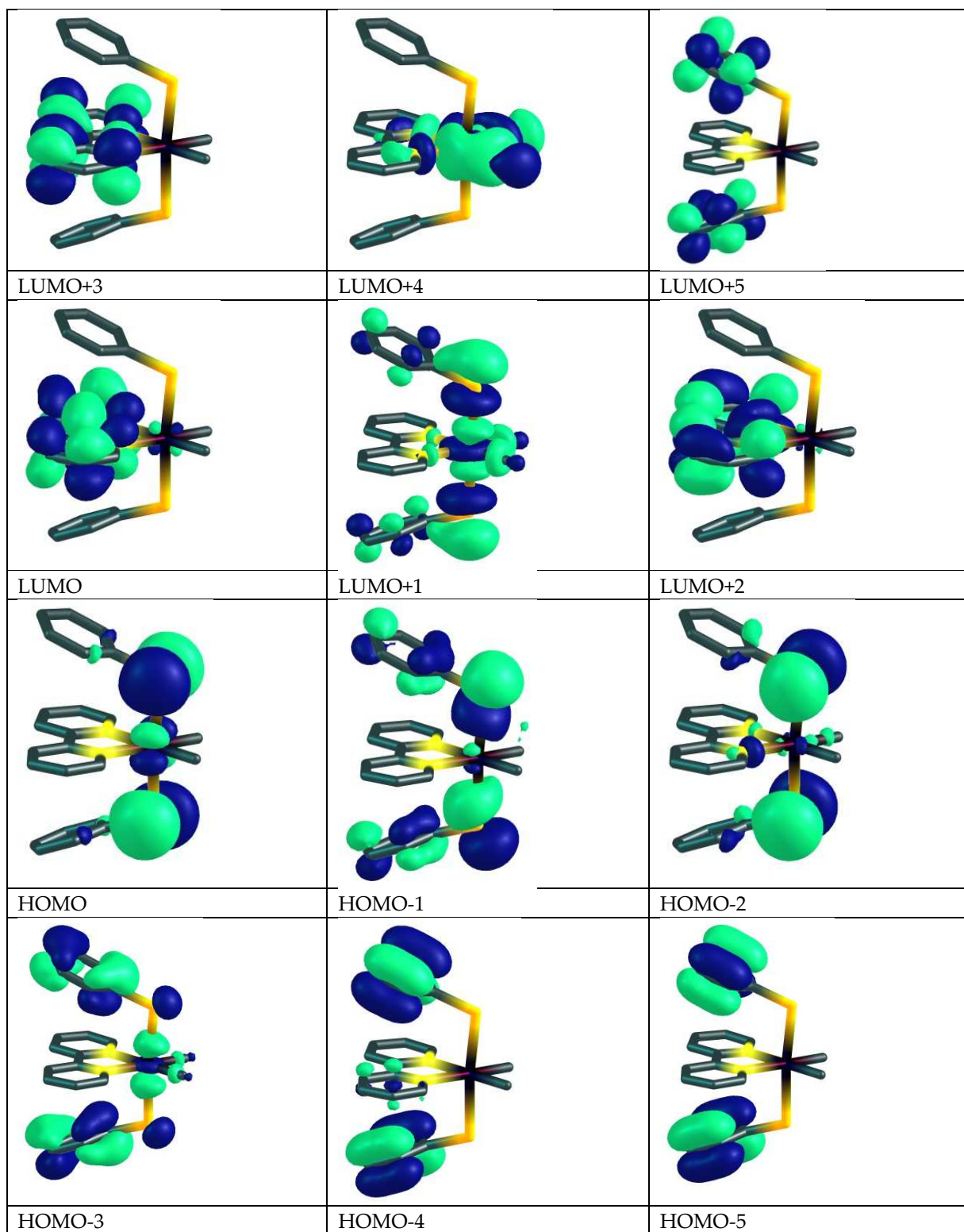


**Figure S11.** Molecular orbital plots for the DFT-optimised  $S_0$  structure of **1b** in  $\text{CH}_2\text{Cl}_2$  solution.

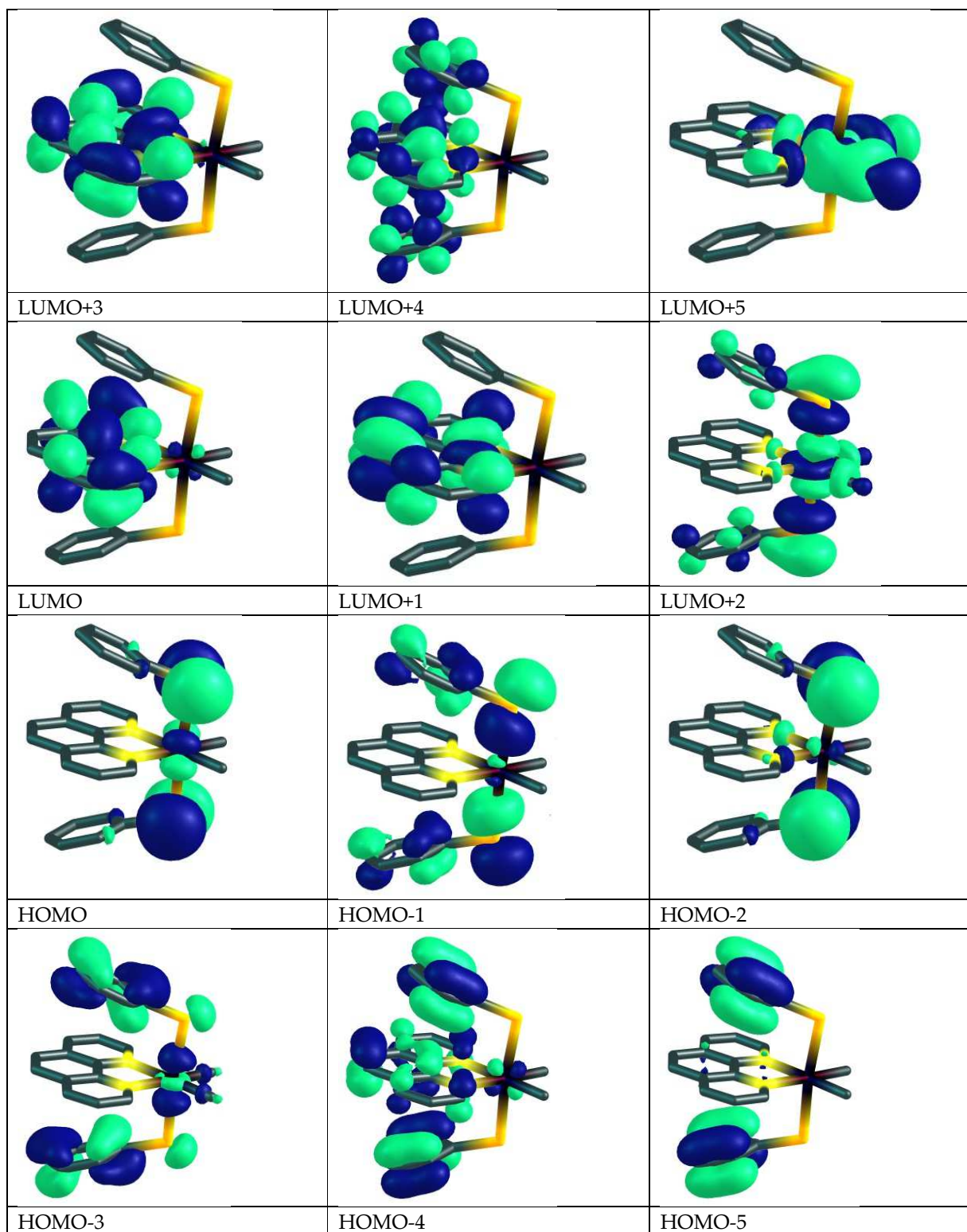


**Figure S12.** Molecular orbital plots for the DFT-optimised  $S_0$  structure of **2b** in  $\text{CH}_2\text{Cl}_2$  solution.

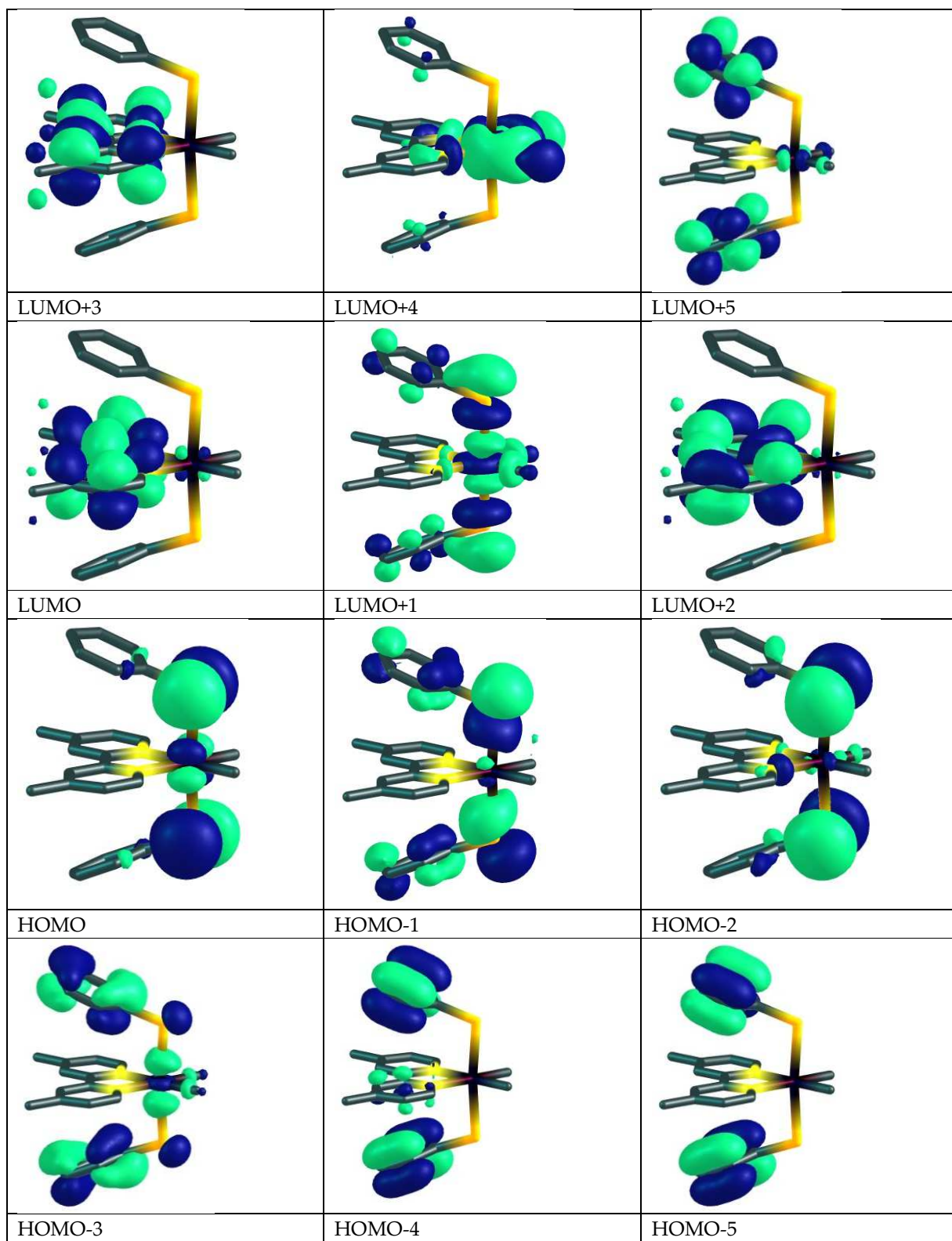


**Figure S13.** Molecular orbital plots for the DFT-optimised  $S_0$  structure of **3b** in  $\text{CH}_2\text{Cl}_2$  solution.

**Table S5.** Composition and energies of selected molecular orbitals of **1b** in CH<sub>2</sub>Cl<sub>2</sub>.

MO	energy (eV)	components(%)				
		Pt	bpy	Se	Ph	Me
LUMO+5	-0.084	5	5	0	89	1
LUMO+4	-0.147	41	25	1	3	30
LUMO+3	-1.101	1	98	1	1	0
LUMO+2	-1.354	3	93	1	3	0
LUMO+1	-1.875	35	3	40	13	9
LUMO	-2.207	2	96	1	1	0
HOMO	-5.316	14	0	74	11	0
HOMO-1	-5.628	12	2	53	32	1
HOMO-2	-5.687	3	5	76	13	3
HOMO-3	-6.768	14	1	71	10	3
HOMO-4	-6.811	0	6	0	94	0
HOMO-5	-6.859	0	2	0	98	0

**Table S6.** Composition and energies of selected molecular orbitals of **2b** in CH<sub>2</sub>Cl<sub>2</sub>.

MO	energy (eV)	components(%)				
		Pt	phen	Se	Ph	Me
LUMO+5	-0.070	4	9	0	86	1
LUMO+4	-0.158	1	64	0	35	0
LUMO+3	-0.861	3	91	1	4	1
LUMO+2	-1.881	35	3	40	13	8
LUMO+1	-2.076	0	99	0	1	0
LUMO	-2.183	2	95	0	1	0
HOMO	-5.318	14	0	74	11	1
HOMO-1	-5.621	12	3	50	34	1
HOMO-2	-5.681	3	6	77	11	3
HOMO-3	-6.762	13	2	10	71	3
HOMO-4	-6.821	0	5	0	95	0
HOMO-5	-6.892	8	57	1	34	0

**Table S7.** Composition and energies of selected molecular orbitals of **3b** in CH<sub>2</sub>Cl<sub>2</sub>.

MO	energy (eV)	components(%)				
		Pt	Me <sub>2</sub> bpy	Se	Ph	Me
LUMO+5	-0.070	8	6	0	82	4
LUMO+4	-0.091	39	25	1	5	30
LUMO+3	-0.936	1	98	0	1	0
LUMO+2	-1.196	2	92	2	3	1
LUMO+1	-1.845	35	3	40	13	9
LUMO	-2.121	1	96	2	1	0
HOMO	-5.290	14	0	74	11	1
HOMO-1	-5.601	12	2	53	32	1
HOMO-2	-5.661	4	5	75	13	3
HOMO-3	-6.748	14	1	11	71	4
HOMO-4	-6.794	0	7	0	93	0
HOMO-5	-6.845	1	2	0	97	0

**Table S8.** Wavelengths and the nature of transitions for the complex **1b**<sup>a</sup>

transition	oscillator strength	calcd. $\lambda$ (nm)	exp. $\lambda$ (nm)	major contribution	assignment
$S_0 \rightarrow S_1$	0.0005	507.17	475	HOMO $\rightarrow$ LUMO (99%)	L'LCT/MLCT
$S_0 \rightarrow S_2$	0.0001	500.07		HOMO $\rightarrow$ L+1 (98%)	IL'CT/L'MCT
$S_0 \rightarrow S_3$	0.0045	443.30	422	H-1 $\rightarrow$ LUMO (79%)	L'LCT/MLCT
$S_0 \rightarrow S_4$	0.0031	438.84		H-2 $\rightarrow$ LUMO (79%)	L'LCT
$S_0 \rightarrow S_5$	0.0015	425.16	372	H-2 $\rightarrow$ L+1 (89%)	IL'CT(n $\rightarrow$ $\pi^*$ )/L'MCT
$S_0 \rightarrow S_6$	0.0014	371.93		HOMO $\rightarrow$ L+2 (100%)	L'LCT/MLCT
$S_0 \rightarrow S_7$	0.9801	354.57	313	H-1 $\rightarrow$ L+1 (86%)	IL'CT(n $\rightarrow$ $\pi^*$ and $\pi\rightarrow\pi^*$ )/L'MCT
$S_0 \rightarrow S_{16}$	0.1042	296.73		HOMO $\rightarrow$ L+4 (76%)	L'MCT
$S_0 \rightarrow S_{22}$	0.1422	282.40		H-6 $\rightarrow$ LUMO (50%), H-5 $\rightarrow$ L+1 (17%)	ILCT IL'CT(n $\rightarrow$ $\pi^*$ )/L'MCT
$S_0 \rightarrow S_{43}$	0.0869	248.32	233	H-7 $\rightarrow$ L+1 (39%) H-1 $\rightarrow$ L+9 (16%) H-9 $\rightarrow$ L+1 (15%)	IL'CT(n $\rightarrow$ $\pi^*$ )/L'MCT IL'CT(n $\rightarrow$ $\pi^*$ )/L'LCT IL'CT(n $\rightarrow$ $\pi^*$ )/LL'CT

<sup>a</sup> M = Pt, L = bpy, L' = SePh and L" = Me. The experimental values *in italics* were not precisely determined (weak shoulders).

**Table S9.** Wavelengths and the nature of transitions for the complex **2b**<sup>a</sup>

Transition	oscillator strength	calcd. $\lambda$ (nm)	exp. $\lambda$ (nm)	major contribution	assignment
$S_0 \rightarrow S_1$	0.0000	500.49	483	HOMO $\rightarrow$ L+2 (85%)	IL'CT(n $\rightarrow$ $\pi^*$ )/L'MCT
$S_0 \rightarrow S_2$	0.0000	500.47		HOMO $\rightarrow$ LUMO (85%)	L'LCT/MLCT
$S_0 \rightarrow S_3$	0.0006	467.29		HOMO $\rightarrow$ L+1 (99%)	L'LCT/MLCT
$S_0 \rightarrow S_4$	0.0088	438.87	372	H-1 $\rightarrow$ LUMO (95%)	L'LCT/MLCT
$S_0 \rightarrow S_5$	0.0010	435.67		H-2 $\rightarrow$ LUMO (95%)	L'LCT/MLCT
$S_0 \rightarrow S_6$	0.0002	426.67		H-2 $\rightarrow$ L+2 (97%)	IL'CT(n $\rightarrow$ $\pi^*$ )/L'MCT
$S_0 \rightarrow S_7$	0.0058	418.46		H-1 $\rightarrow$ L+1 (99%)	L'MCT
$S_0 \rightarrow S_8$	0.0006	411.80		H-2 $\rightarrow$ L+1 (100%)	IL'CT(n $\rightarrow$ $\pi^*$ )/L'MCT
$S_0 \rightarrow S_9$	0.9711	356.50	319	H-1 $\rightarrow$ L+2 (95%)	L'MCT
$S_0 \rightarrow S_{22}$	0.0561	293.19	272	HOMO $\rightarrow$ L+5 (65%)	IL'CT(n $\rightarrow$ $\pi^*$ )
$S_0 \rightarrow S_{36}$	0.1357	267.82	232	H-7 $\rightarrow$ LUMO (31%) H-8 $\rightarrow$ L+1 (26%)	ILCT/MLCT L'LCT/MLCT

<sup>a</sup> M = Pt, L = phen, L' = SePh and L" = Me. The experimental values *in italics* were not precisely determined (weak shoulders).

**Table S10.** Wavelengths and the nature of transitions for the complex **3b**<sup>a</sup>

transition	oscillator strength	calcd. $\lambda$ (nm)	exp. $\lambda$ (nm)	major contribution	assignment
$S_0 \rightarrow S_1$	0.0001	499.00	478	HOMO $\rightarrow$ L+1 (98%)	IL'CT(n $\rightarrow$ $\pi^*$ )/L'MCT
$S_0 \rightarrow S_2$	0.0005	493.58	424	HOMO $\rightarrow$ LUMO (99%)	L'LCT/MLCT
$S_0 \rightarrow S_3$	0.0062	433.69		H-1 $\rightarrow$ LUMO (85%)	L'LCT/MLCT
$S_0 \rightarrow S_4$	0.0038	428.93	379	H-2 $\rightarrow$ LUMO (84%)	L'LCT/MLCT
$S_0 \rightarrow S_5$	0.0018	424.61	371	H-2 $\rightarrow$ L+1 (87%)	IL'CT(n $\rightarrow$ $\pi^*$ )/L'MCT
$S_0 \rightarrow S_6$	0.0090	357.71		HOMO $\rightarrow$ L+2 (99%)	L'LCT/MLCT

$S_0 \rightarrow S_7$	0.9817	353.81	314	H-1 → L+1 (83%)	IL'CT( $n \rightarrow \pi^*$ and $\pi \rightarrow \pi^*$ )/L'MCT
$S_0 \rightarrow S_{16}$	0.0981	296.05		HOMO → L+4 (49%)	L'LCT/L'MCT
$S_0 \rightarrow S_{21}$	0.0211	283.48		H-3 → L+1 (57%)	IL'CT( $n \rightarrow \pi^*$ and $\pi \rightarrow \pi^*$ )/L'MCT
$S_0 \rightarrow S_{43}$	0.0439	248.09	234	H-4 → L+1 (12%)	IL'CT( $n \rightarrow \pi^*$ and $\pi \rightarrow \pi^*$ )/L'MCT
				H-12 → L+1 (74%)	ML'CT/IL'CT( $n \rightarrow \pi^*$ )

<sup>a</sup> M = Pt, L = Me<sub>2</sub>bpy, L' = SePh and L" = Me. The experimental values *in italics* were not precisely determined (weak shoulders).

## References

- (1) A. J. Carty, H. Jin, B. W. Skelton, A. H. White, Oxidation of Complexes by (O<sub>2</sub>CPh)<sub>2</sub> and (ER)<sub>2</sub> (E = S, Se), Including Structures of Pd(CH<sub>2</sub>CH<sub>2</sub>CH<sub>2</sub>CH<sub>2</sub>)(SePh)<sub>2</sub>(bpy) (bpy = 2,2'-Bipyridine) and MM<sub>2</sub>(SePh)<sub>2</sub>(L<sub>2</sub>) (M = Pd, Pt; L<sub>2</sub> = bpy, 1,10-Phenanthroline) and C···O and C···E Bond Formation at Palladium(IV), *Inorg. Chem.* **1998**, *37*, 3975–3981.
- (2) K.-T. Aye, J. J. Vittal, R. J. Puddephatt, Oxidative addition of E–E bonds (E = Group 16 element) to platinum(II): a route to platinum(IV) thiolate and selenolate complexes, *J. Chem. Soc., Dalton Trans.* **1993**, *1993*, 1835–1839.